京都大学防災研究所年報 第 58 号 B 平成 27 年 6 月
Annuals of Disas. Prev. Res. Inst., Kyoto Univ., No. 58 B, 2015

Numerical Simulation for the Erosion and Stability of Riverbanks Subjected to Different Flood Hydrographs

Ahmed ALY EL-DIEN, Hiroshi TAKEBAYASHI, and Masaharu FUJITA

Synopsis

Stability of riverbank under the conditions of five different flood hydrographs and of three bed conditions is discussed using the results of numerical simulation. Three models of hydraulic fluvial erosion, seepage flow, and slope stability are coupled to discuss the effect of the seepage flow and river bed deformation on riverbank stability. The fluvial erosion model predicts the distribution of boundary shear stress along the river cross section and then predicts the erosion progress. The seepage model predicts the spatial and temporal variations in the groundwater table and the pore-water pressure inside the riverbank. Stability model calculates the factor of safety of bank material and estimates the possible failure plane. The three models are based on the finite element method with moving boundaries. The response of riverbank to the oscillated water level in the river and the consequent groundwater table is analyzed. The trend of factor of safety through time is presented. The influence of relevant geometrical, internal and external forces are also discussed.

Keywords: Riverbank stability, flood, seepage, fluvial erosion, hydrograph.

1. Introduction

Flood characteristics such as magnitude, frequency, duration, peak discharge, and variability govern some aspects of the river as they erode, transport and deposit sediments in the river reach.

Stability of riverbank depends on its geometry, its material properties, and the forces to which it is subjected. These forces include the effects of water both internally, in the form of pore-water pressure and seepage forces and externally in terms of confining water pressure and hydrodynamic forces (Lane and Griffiths, 2000). The movement of water through voids generates a hydraulic drag in the direction of flow which is known as seepage force. Seepage force is generated when hydraulic head gradient exists between two points within the saturated zone. The seepage force acts to separate the soil particles and reduces the effective stress. Many banks are frequently subjected to sudden changes of water level (rise or fall), like the riverbanks during flood events, reservoir banks during dam operation, and irrigation channels that are operated by rotation system. In a two-turn rotation irrigation system, the agricultural land is divided into two parts. The branch channels that serving the first part are "working" and allowed to convey water with full capacity while the other channels that serving the second part are "closed" with no flow. The two-turn rotation is reversed after 8 days (4 working + 4 closing) and so on, such rotation irrigation system is commonly used in Egypt. In this system there is a periodic filling and emptying for the channels which affect the stability of its banks. Such fluctuation in water level alters the hydraulic conditions inside the bank and finally leads to bank failure. Bank retreat occurs by a combination of two processes: (1) hydraulic fluvial

erosion by the erosive stress of the flowing water and it acts mainly on the lower portion of the bank, (2) mass failure under gravity which occurs on the upper part of the bank.

Fluvial erosion is caused by an imbalance between hydraulic shear stress on the bank surface and the resistance of a bank material. When the shear stress exceeds the critical shear strength of the bank material, hydraulic erosion processes are initiated. Mass failure occurs if there is a change in the bank geometry or a change in the applied loads. During flood event, a great amount of sediment is removed from the bank toe and bed (change in geometry), the bank becomes too steep and, maybe, an overhang is formed. Such alteration in the geometry changes the distribution of normal and shear stresses inside the riverbank. Also, any increase in the bank weight due to saturation or external loads will also change the stress distribution. Mass failure takes place when the generated stresses reach certain failure criterion that depends on cohesion c' and angle of friction ϕ' for riverbank material. It have been found that mass failure takes place as a second step after the hydraulic erosion forms a deep undercut at the bank toe (Thorne, 1982; Darby et al., 2010).

Beside the erosive shear stress, field studies have found other flow properties to be more strongly correlated to hydraulic erosion during flood events. For example, (Wolman, 1959) found a relation between the storm duration and the hydraulic erosion. (Knighton, 1973) found that flow variability (number of discharge peaks) also affects bank erosion. (Hooke, 1979) showed that at sites where hydraulic processes are dominant over sub-aerial processes, the variable with the strongest correlation to bank erosion is event peak discharge. (Julian and Torres, 2006) found that event peak of excess shear stress is the best predictor of bank erosion for moderately cohesive banks and variability of excess shear stress is the best predictor for minimally cohesive banks. They concluded that hydraulic bank erosion is dictated by flood peak intensities.

The flood event changes the internal forces inside the riverbank. For example, during the high water surface level (WSL) resulted from the flood, the banks are saturated and its weight become heavier than before, and also internal seepage flow generates seepage forces in addition to the generation of positive pore water pressure.

The objective of this paper is to (1) investigate the response of riverbanks under different flood events and determine the most critical flood pattern, (2) achieve a better understanding for the factors and mechanisms determining bank stability; and (3) to investigate interactions between fluvial erosion processes and mechanisms of mass failure in controlling bank morphology.

This research tries to investigate to what extent a flood event can affect the riverbank on two main aspects: (1) the change in bank geometry, (2) the change in forces. To assess the change in geometry, fluvial erosion model is presented. To evaluate the internal pore water pressure, the seepage model is presented. Finally, results from both the erosion and seepage models are incorporated into a stability model to calculate the factor of safety (FOS) and predict the expected failure plane. Stability of hypothetical riverbank subjected to five different flood hydrographs and three bed conditions is numerically simulated. First we briefly describe the formulations for fluvial erosion, seepage flow and riverbank stability models. Subsequently, the effects of flood hydrograph characteristics and the results from simulation cases are discussed. Finally, we conclude our findings and outline the limitations in our approach to be considered in the future research.

2. Models

2.1 Fluvial Erosion model

The rate of fluvial bank erosion can be quantified using an excess shear stress formula (Osman and Thorne, 1988; Langendoen and Simon, 2008):

$$\omega = k(\tau_o - \tau_{cr})^{\beta} \qquad \text{if} \quad \tau_o > \tau_{cr} \qquad (1\text{-a})$$

$$\omega = 0.0 \qquad \text{if} \quad \tau_o \leq \tau_{cr} \qquad (1\text{-b})$$

where ω is the eroded distance normal to the bank surface per unit time (m/sec), τ_o is the shear stress from flow (N/m^2), k is the erodibility coefficient ($m^3/N{\cdot}s$); τ_{cr} is the critical shear stress for entrainment (N/m^2); and$\beta$is an empirically derived

exponent (dimensionless), often assumed to have a value of 1.0 in bank erosion studies, (Rinaldi and Darby, 2007). Erosion distance perpendicular to the bank surface, E, can be calculated from:

$$E = \omega \times \Delta t \quad (2)$$

Where E in (m), and Δt is the time step (second). The fluvial erosion model requires the determination of the three parameters τ_o, k, τ_{cr}.

The acting boundary shear stressτ_o, is estimated using the flow net method described by (Guoliang Yu., and Soon-Keat, 2007). The distribution of boundary shear stress τ_o is calculated each time step according to the new updated geometry and flow conditions. Erodibility coefficients k, τ_{cr} depends on the type of bank material and can be measured by different devices such as the erosion function apparatus, the submerged jet test device, and by means of straight or annular flume tests, (Briaud et al., 2001). Erosion progress through the bank is predicted by using two conjugate adaptive finite element meshes. The fluvial erosion model that simulates the temporal and spatial changes in the profile of cohesive riverbanks is explained in details by (Aly El-dien et al., 2013). Erosion model is based on the following two assumptions:(1) The river is straight which means there is no secondary flow, (2) The bank material is cohesive and relatively homogeneous, which means that erosion advancement is synchronized in both bed and banks according Eq.(1), (2) above. Deposition process is not incorporated in the model. Accordingly, aggradation/degradation model based on solving the sediment continuity equation, sediment transport equation, should be applied to estimate the amount of bed erosion.

2.2 Seepage model

The finite element seepage model introduced by (Gottardi, and Venutelli, 2001) is employed to simulate 2-D transient saturated-unsaturated seepage flow through the riverbanks. The governing equation for water flow through saturated and unsaturated soil can be obtained by introducing Darcy's law into the mass continuity equation. The general governing differential equation for two-dimensional seepage is given by Richard's equation as:

$$\frac{\partial}{\partial x}\left(K_x(\psi)\frac{\partial \psi}{\partial x}\right) + \frac{\partial}{\partial z}\left(K_z(\psi)\left(\frac{\partial \psi}{\partial z} + 1\right)\right) = C(\psi)\frac{\partial \psi}{\partial t} \quad (3)$$

where ψ is the pressure head, [L]; $K_x(\psi)$, $K_z(\psi)$ are the unsaturated hydraulic conductivity in x, z directions respectively, [LT^{-1}]; $C(\psi) = \partial\theta/\partial\psi$ is the specific water capacity, [L^{-1}]; θ is the volumetric water content [L^3L^{-3}], $\theta = nS$; n is the soil porosity; S is the degree of saturation (S ranges from 0.0 in dry soil to 1.0 in fully saturated soil); x, z are the horizontal and the vertical coordinates, respectively, [L]; and t is time, [T].

In an unsaturated soil, both the volume of water stored within the voids, and hydraulic conductivity will vary depending on the negative pore-water pressure. A conductivity function ($K-\theta$ curve) and a storage function ($\psi-\theta$ curve) should be well defined to complete the seepage model. These two functions could be obtained, for every soil type, by direct measurement in the laboratory and then inserted into the seepage model to get $K(\psi)$ and $C(\psi)$. Since it can sometimes be difficult or time consuming to obtain the storage and conductivity functions by laboratory measurements, the functions could be estimated by using closed-form solutions as proposed by (Van Genuchten, 1980) or (Fredlund and Xing, 1994). Essential assumption in the analysis of seepage model is that the initial pore water is assumed to vary hydrostatically with distance above or below the groundwater table. That is, pore-water pressure is negative and decreases linearly above the groundwater table, and conversely below the groundwater table pore-water pressure is positive and increases linearly, the same approach as (Rinaldi and Casagli, 1999).

2.3 Stability Model

Riverbank stability can be performed using either the traditional limit equilibrium methods such as the Bishop's modified method, Janbu's generalized procedure of slices, and Spencer's method (Duncan, 1996) or by using the numerical deformation finite element methods such as the gravity increase method (Swan and Seo, 1999) and the strength reduction method (Matsui and San, 1992; Griffiths and Lane, 1999).

The stability model in the current study is a finite element elastic-plastic deformation model

that uses the strength reduction technique. Shear strength of bank material is proportional to cohesion c' and angle of friction ϕ' and the stability of the banks increases with an increase in c'andϕ'. In the strength reduction technique the original shear strength parameters c' , ϕ' are virtually reduced by dividing by a strength reduction factor (SRF) in order to bring the slope to the point of failure (Smith and Griffiths, 2013). The factored shear strength parameters c'_f, and ϕ'_f are therefore given by:

$$c'_f = c'/SRF$$
$$\phi'_f = \arctan(\tan\phi'/SRF) \quad (4)$$

The factor of safety for the slope is equal to the strength reduction factor (FOS=SRF) when failure takes place. Stability model consists of three sub-models:(1) plane strain model to calculate the shear and normal stress distribution inside the riverbank, (2) Mohr-Coulomb failure model to determine which nodes have been yielded and overstressed, and (3) elastic-plastic algorithm to redistribute the stresses of yielding nodes through the mesh. Detailed explanations are given by (Smith and Griffiths, 2013).

3. Numerical Simulation

3.1 Hydraulic Conditions

Five flood hydrographs having the same runoff volume but with different patterns are assumed to pass through the river cross section as shown in Fig.1. Base time of Hyd-1is double that of Hyd-2 and it has constant peak discharge equals half the value of Hyd-2. Hyd-3 simulates the early peak flood event (rapid increase and gradual decrease) while conversely Hyd-4 simulates the late peak one .Hyd-5 is a multiple peak hydrograph. The maximum peak discharge is 600 m^3/secand the base time lasts for 10 days except for Hyd-1 and Hyd-2 to satisfy the constant runoff volume criterion. In order to study the effect of fluvial hydraulic erosion, three bank-bed conditions are assumed; first the case of "No-erosion"; second the case of "Fixed-bed" where the bed material is so rigid that the stream cannot pick it up during flood and hence the banks only are attacked by the flowing water; third the case of "Movable-bed" where both banks and bed erodes simultaneously.

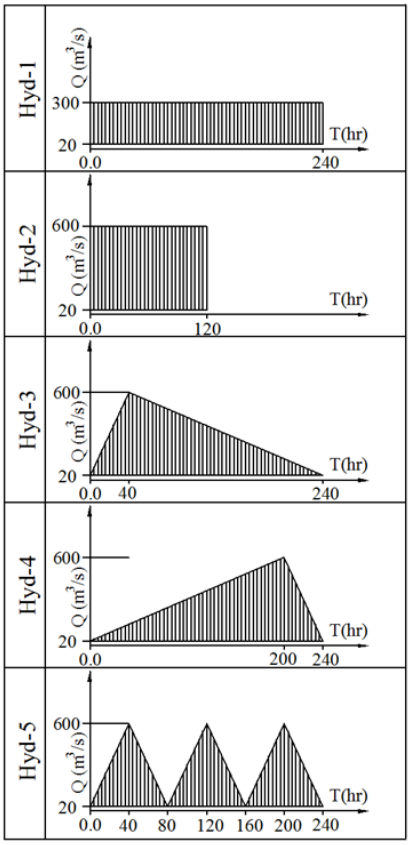

Fig.1 Patterns of flood hydrograph

3.2 Hypothetical data, Initial and boundary conditions

Typical riverbank with dimensions as shown by Fig.2 is considered. Shear strength parameters of bank material can be determined by results of direct and tri-axial shear tests, but we use hypothetical data with similar range to those published before.$c' = 12\ KN/m^2$, $\phi' = 20^\circ$, Young's modulus $E = 1 \times 10^5\ KN/m^2$ and Poisson's ratio $\nu = 0.3$, dilation angle, $\psi^* = 0^\circ$, and the saturated permeability $k_x = k_y = 1.389^{-5}$ m/sec , porosity= 0.43, S_s (specific storage) = 10-5 m^{-1}, γ soil(under GWT) $= 20\ KN/m^3$, γ soil(above GWT) $= 18\ KN/m^3$, $\tau_{cr} = 1.2\ KN/m^3$, $k = 3.6 \times 10^{-7} m^3/N.sec$, S_b(bed slope) = 0.0005 , n (manning coefficient) = 0.015. Initial GWT is assumed horizontal at the same level of WSL at the beginning of the hydrograph. Pore-water pressure (PWP) under the

GWT is initially assumed as hydrostatic pressure as shown by Fig. 2. The conductivity function ($K-\theta$ curve) and a storage function ($\psi-\theta$ curve) for the riverbank silt soil are drawn from the data obtained by (Gottardi and Venutelli, 2001) as shown by Fig. 3.

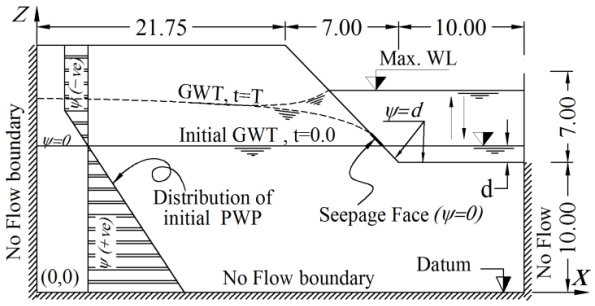

Fig.2 Dimensions and boundary conditions of seepage model

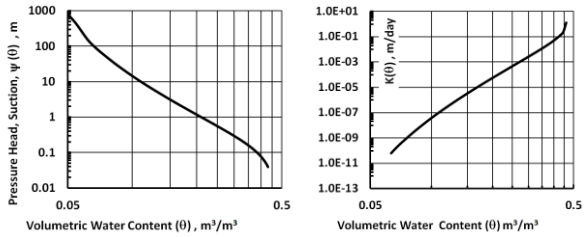

(a) (b)

Fig.3(a)Storage function ($\psi-\theta$ curve) , (b) Conductivity function ($K-\theta$ curve)

3.3 Treatment of hydrograph and the dynamic boundary conditions

Ten simulation days are divided into sixty time periods each of 4-hours period. Flood discharge is considered constant during each time period and the corresponding WSL is calculated by iterative procedure using Manning equation. For every time step and for the newly updated geometry of the riverbank, the seepage model is run and the GWT is obtained, finally the factor of safety (FOS) is calculated and the expected plane of failure is determined by the stability model. The above mentioned procedure is repeated each time step until the required simulation time is reached.

Each new time period requires three boundary conditions from the previous step: (1) the newly updated bank geometry, and (2) the initial pore water pressure (PWP) for step *i* is the resulting PWP from step *i-1*. (3) specified pressure head. WSL is very important to define the specified head boundary condition for seepage model, and the force vector in the stability model. In the stability model, the horizontal displacement is zero for the two vertical sides, but both the vertical and horizontal displacements are zero for the lower boundary. The force vector represents the equivalent nodal gravity weight, and confining water pressure. Pore water pressure is interpolated from the seepage model and found at each gauss point then subtracted from the total stress to get the effective stress in the stability model. Mesh and boundary conditions for plane strain stability model are shown in Fig. 4

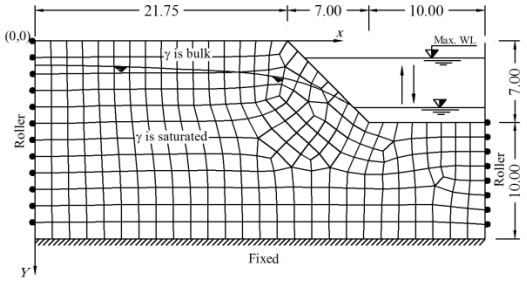

Fig.4 Mesh and boundary conditions of stability model.

4. Results and Discussion

In the following paragraphs we will discuss how floods can affect the geometry and both external and internal forces. Three factors influence the stability of the river bank: (1) Change in the geometry. (2) Change with the WSL (external force). (3) Change of the GWT (internal force). It should be considered that the factor of safety (FOS) is calculated even it is less than 1.0 in order to investigate the trend of FOS. In the following, we discuss each of them in details.

4.1 Effect of flood on the riverbank geometry (width, depth, slope):

Flow characteristics are governed by the existing river dimensions, shape, slope and bed roughness but these may themselves be altered by

the flow, especially during floods. As long as discharge remains below the competent threshold the cross-section shape formed by the last flood remain unchanged and governs the flow characteristics.

A change in the geometry of the bank may occur when the streambed lowers or degrades due to the instability of the stream system. Generally, fluvial erosion caused by floods (1) makes the river cross section to become wider and deeper which increases the bank height, (2) steepen the bank slopes,(3) helps the formation of overhangs.

(1) Formation of overhangs

Geometry of the riverbank subjected to the different flood cases is shown by Fig.5. By comparing the "fixed-bed" cases to "movable-bed" cases, an overhang or deep cut near the bank toe is most likely to be formed in the "fixed-bed" cases. One reason is that the flow energy is resisted by the rigid bed and the other part strongly attacks the banks, so the final result is erosion in the bank toe. When the WSL remains constant for a period of time, the flow erodes the same wetted perimeter and removes particles which finally form an overhang.

Overhang is also formed in the "movable-bed" case of Hyd-4, because the WSL changes very slowly or almost constant. Bed condition and existence of armor layers controls the stability of banks. Formation of overhang is a function of the rigid bed and the time variation of WSL. Overhanging conditions can only occur in cohesive riverbanks, and they are inherently unstable and can fail with only slight changes in the bank conditions.

(2) Change in depth and width

Although the discharge of Hyd-2 is double the discharge of Hyd-1, the base time of Hyd-2 is half the base time of Hyd-1. The volume of water passing through the river cross section is equal whether from Hyd-1 or from Hyd-2. Fig.6 shows how the hydrograph pattern affects the geometric shape of the river cross section. The river cross section is wider and shallower in case of Hyd-2.

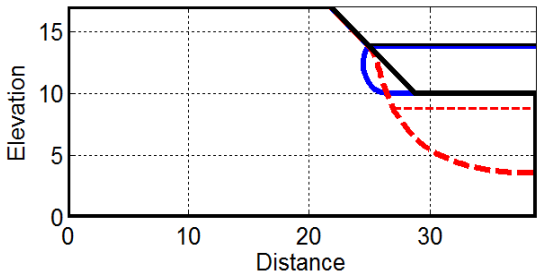

(a) Hyd-1

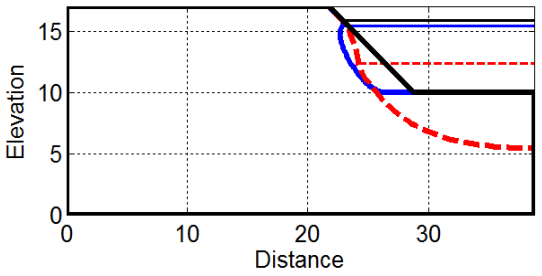

(b) Hyd-2

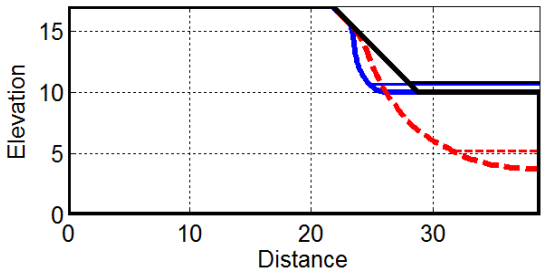

(c) Hyd-3

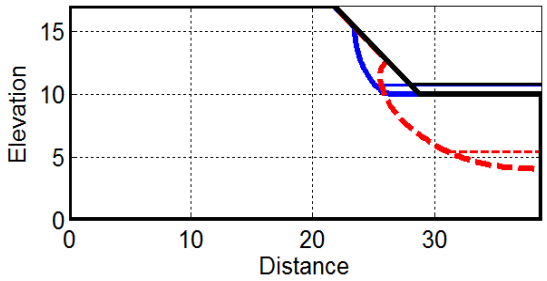

(d) Hyd-4

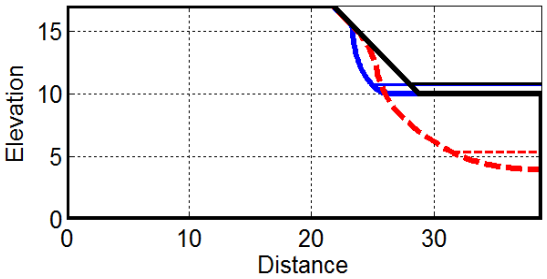

(e) Hyd-5

Fig. 5 Bank profile for different flood events.

Fixed bed case; Movable bed case

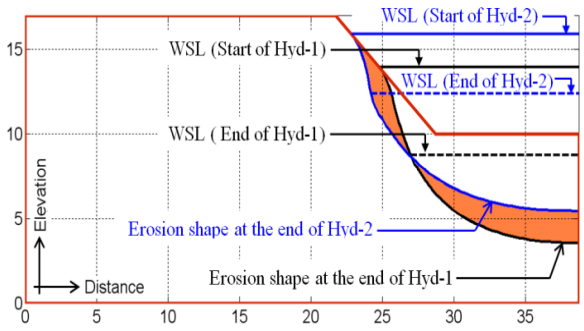

Fig.6 Effect of flood on width and depth of river x-sec. Results after simulation time of 10 days

Since the discharge of Hyd-2 is double the value of Hyd-1, the water depth and hydraulic radius of case Hyd-2 are greater than those for case Hyd-1. As a result, a long portion of the wetted perimeter on the bank side is subjected to friction and sheared by the flow, this leads to the lateral erosion of the bank and widen the channel. But in case Hyd-1, the water depth is small and the wetted perimeter of the bank is short, so the widening effect is not significant. The boundary shear stress produced by Hyd-2 is greater than that produced by Hyd-1 as shown by Fig.7, so it is expected that the erosion depth accompany Hyd-2 is much deeper than the erosion depth from Hyd-1, which holds true if both hydrographs have the same base time. But the base time of Hyd-2 is only half that of Hyd-1 and the channel widening makes the shear stress smaller which explain why the erosion depth of Hyd-1 is deeper than the erosion depth of Hyd-2.

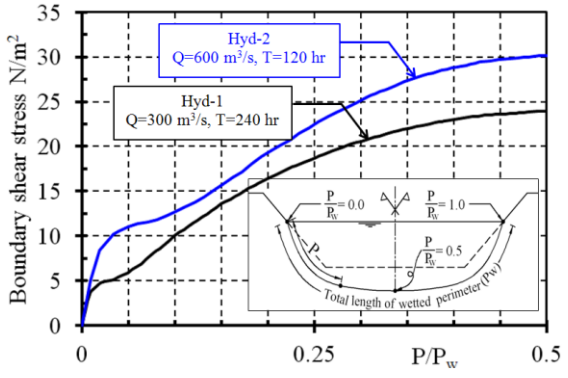

Fig.7 Boundary shear stresses at the end of Hyd-1 and Hyd-2.

(3) Cumulative erosion volume

Fig.8 shows temporal change of cumulative erosion volume. There is no significant difference of the final cumulative erosion volume except for Hyd-2. It is thought that the reason for being wider and shallower mentioned above makes this difference. Erosion volume per unit length of river increases uniformly for cases of constant discharges (Hyd-1 and Hyd-2) and increases with an increasing rate during the rising stage of the hydrograph, and inversed at the peak discharge to increases with a decreasing rate during the recession hydrograph stages.

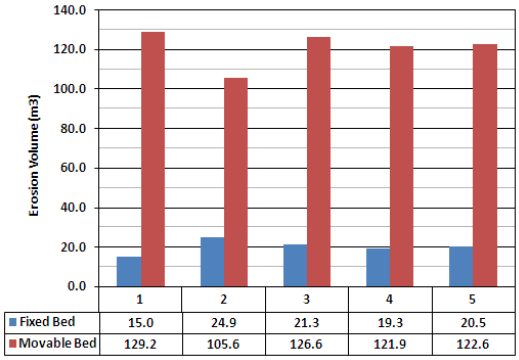

Fig.8 Erosion volume at the end of each hydrograph

(4) Change in water surface level

Fig. 9 shows the change in water surface level in the river for the five flood hydrographs. The WSL increases during the rising stage of the hydrograph and decrease with its recession stage which matches the logic sense. But in case of movable bed of Hyd-4, the WSL remains constants although during the rising stage because of the synchronized increase in the discharge and the degradation in bed area as shown by Fig.9-e.

From the above discussion, it can be concluded that long-term changes in discharge magnitude or duration have important implications for channel form and process. River width and depth depend on discharge value and material characteristics. Width increases faster than depth for high discharges. The flood events with small discharge and long duration cause greater erosion volumes than floods with high discharge and short duration if they are of the same runoff volume.

Field observations by (Wolman, 1959) found that maximum bank erosion occurred during winter months. Winter storms were longer in duration and of less intensity than summer storms. Wolman's observations match reasonably our results.

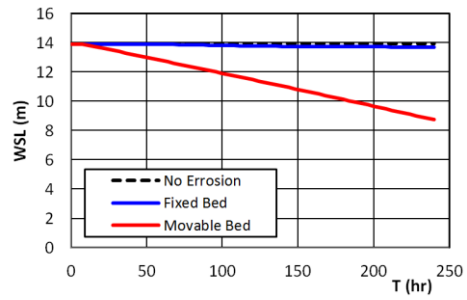

(a) Hyd-1

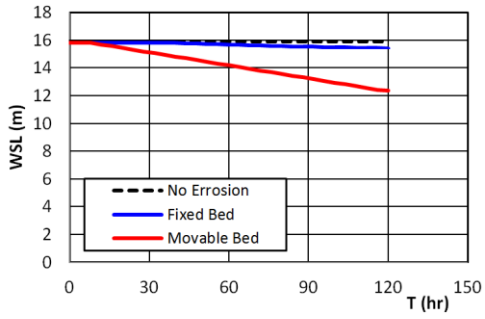

(b) Hyd-2

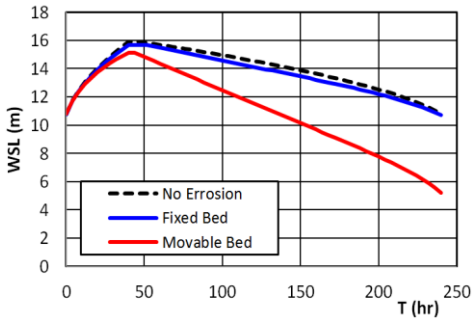

(c) Hyd-3

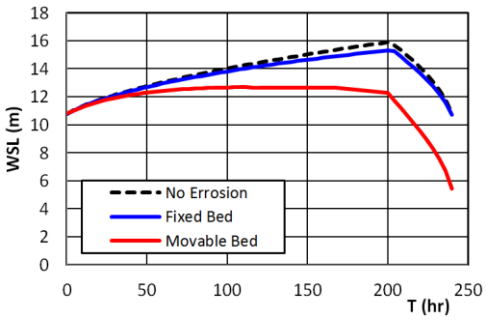

(d) Hyd-4

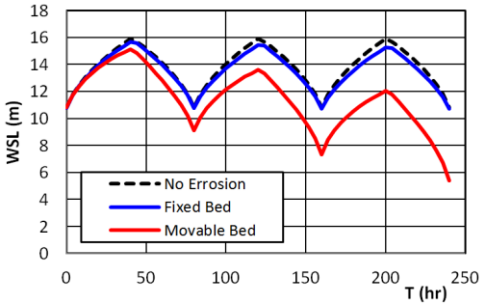

(e) Hyd-5

Fig.9 Variation of WSL for different flood events

(Knighton, 1973) found similar results as Wolman's, but added that flow variability (number of discharge peaks) also affects bank erosion. Knighton inferred that in addition to their longer durations, winter storm-flow events caused a much greater amount of erosion because of their multiple peaks as compared to summer storm-flow events which had single peaks which also agrees well with our results.

4.2 External factors affecting the riverbank stability:

Both the confining pressure produced by the water in the river and the soil mass at the toe of the bank are denoted as external factors that affect the riverbank stability in this section. The trend of factor of safety through time is shown by Fig.10. During the rising stage of flood events, the WSL increases and the factor of safety increases as a consequence of the stabilizing confining pressure of the water in the river.

During the rescission stage, the WSL drops down in the river and the confining pressure in the river decreases making the factor of safety falls to lower values than those experienced before. It is clear from any of the five cases in Fig.10 that at a certain time, the FOS for the case of "No-erosion" is higher than the case of "Fixed-bed" which is also much more stable than the case of "Movable-bed". For example, at time 72 hour in Hyd-3 the FOS changes from 1.62 for the No-erosion case to 1.46 for the "Fixed-bed" case to 1.22 for the "Movable-bed" case. The removed material and the eroded toe of the bank reduce the gravity forces resisting failure so that the computed factor of safety reduces progressively. It should be noticed that the FOS decreases rapidly at the start of the calculation in Hyd-1 and Hyd-2 because the GWT inside the bank is initially assumed below the WSL in the river, and with the passing time the GWT rises while the WSL remains almost constant or slowly drops down as shown by Fig.9. This action accelerates the instability condition inside the bank. However, in the other cases, Hyd-3 to Hyd-5, the rising discharge is accompanied by a slight rise in the WSL and produces an outer confining pressure great and fast enough to compensate the generated inner pore pressure.

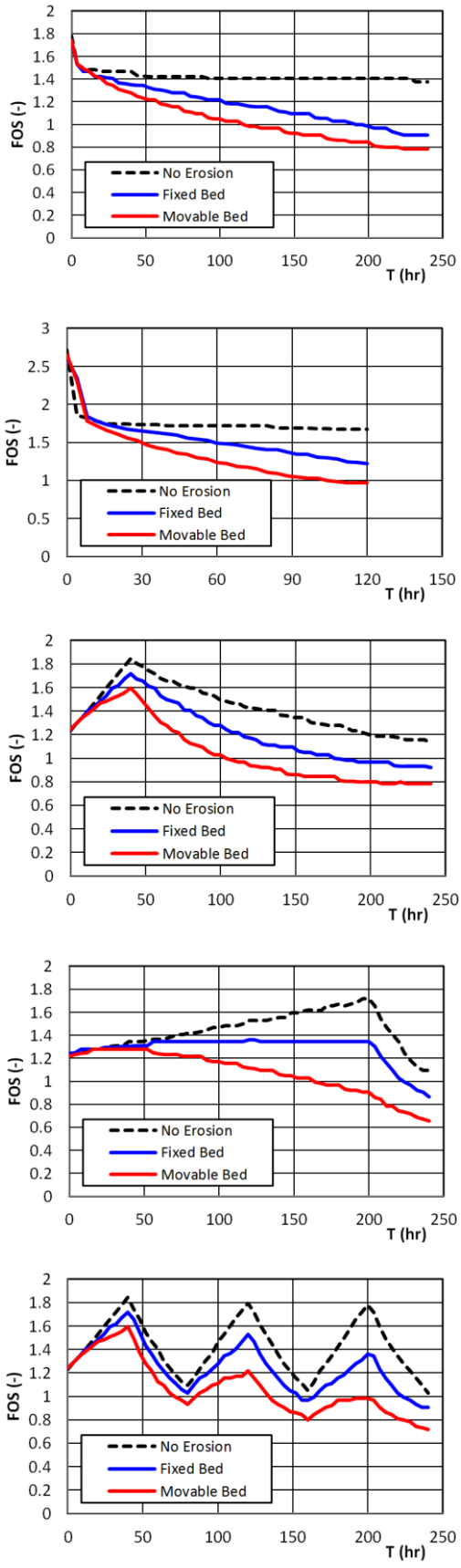

Fig.10 Variation of FOS for different flood events

The earliest failure is noticed to occur during flood Hyd-5 (after 156 hr for "Fixed-bed" case and after 72 hr for "Movable-bed" case). While the latest bank failure occurs under flood Hyd-4 (after 224 hr for "Fixed-bed" case and after 164 hr for "Movable-bed" case). In the "No-erosion" case, the bank is stable under all hydrograph patterns. The slow erosion rate (deformation) and slow variation in the WSL are thought to be the cause of delayed failure under the effect of Hyd-4, while the very rapid variation in WSL (and consequently the GWT) under the effect of Hyd-5 accelerates the failure.

In the multiple peak hydrograph, Fig.10-e, sharp peaks in FOS values reveal that the peaks of flood events have crucial effects on bank stability. During the rising stage of each flow event, FOS increased abruptly and during the drawdown it falls, reaching lower values than those exhibited prior to the event.

4.3 Internal factors affecting the riverbank stability:

Pore water pressure (PWP) and the mechanical properties of bank material are denoted as the internal factors that affect the riverbank stability in this section.

(1) Change of the mechanical properties of bank material

When the GWT rises up, a significant positive pore water pressures is generated and the bank is gradually saturated. Such saturation reduces the contact between soil particles and then the internal friction angle ϕ' is reduced. Besides, saturation affects the chemical bonds between particles and reduces the apparent cohesion c'. Moreover, saturation increases the unit weight of bank material. Finally, saturation reduces the effective stress. All the above four negative effects of saturation are against the stability of the bank and may cause the factor of safety to become less than 1.0. However, the stabilizing effect of the confining pressure from the water in the river may counterbalance the destabilizing effects of saturation.

During the rising hydrograph stage, there are two opposite actions on the riverbank. First, the confining pressure acting on the riverbank face stabilizes the riverbank and increase the FOS.

Second, the raising-up free surface or (GWT) increases the field of positive pore water pressure inside the bank which reduces the FOS. During the rescission hydrograph stage these two actions are conversely changed.

(2) Effect of peak time of the flood

In most cases in Fig.10, failure occurs during recession stage or some hours after the flood peak. But this is not a governing rule because as we see in the case of "Movable-bed", the failure in Hyd-3 occurs during the recession stage while the failure in Hyd-4 occurs during the rising stage. Although the discharge continues to increase during the rising stage of Hyd-4, the WSL remains almost constant because the bed and banks continues to degrade. This situation changes the bank geometry (increase height, steepen its slope). The main reason of failure is only the geometry change in this case because there is no significant variation in GWT. The fluvial erosion is very active while the confining water pressure remains constant while the sever degradation continuous to progress.

(3) Effect of recession rate on bank stability

Comparing the case of "Movable-bed" in both Hyd-3 and Hyd-5, the water surface level drawdown rate in Hyd-3 is about 5 cm/day while in Hyd-5 is about 15 cm/day as shown from Fig.9. After 72 hours the riverbank collapses under the effect of Hyd-5, while the FOS is still 1.22 under the effect of Hyd-3. On the other hand, at the failure time the volume of eroded material under the effect of Hyd-3 is about 24.4 m^3 while under the effect of Hyd-5 is about 20.36 m^3. In this case, it is intelligible that the failure doesn't occur by geometric change.

The stability of riverbank during recession stage of the hydrograph is greatly influenced by how fast its pore water drains. If rapid recession rate took place while the riverbank remains saturated, at least for a while, this condition induces a reduction in the confining pressure outside the riverbank but the GWT is still high inside it. During high recession rate, WSL drops rapidly while the GWT falls slowly (depending on the hydraulic conductivity of the bank material) so that a pressure difference is generated between outside and inside the riverbank which is supposed to be the cause of failure. Rapid drawdown causes this difference to be high. Slow drawdown causes the pressure difference to be small.

In the multiple peak hydrograph, during recession stages, the GWT drops down at a slower rate than WSL drops. The FOS is expected to increase again in two conditions 1) the rise-up of the WSL, 2) the dropdown of the GWT and the bank is expected to restore its stability after totally draining the inside water. Generally, its severity is a function of the time that the GWT remains high. These results are consistent with (Rinaldi et al. 2004)

(4) Seepage flow field and directions

The direction of seepage flow depends mainly on the relative difference in water level between inside and outside the riverbank. Generally, the direction seepage flow changes from an inward direction during rising stage to an outward direction during recession stage. Seepage force (hydraulic drag which results from the movement of water through pores) acts in the same direction of seepage flow. This force is expected to (1) cause local scour and piping (for non-cohesive material) or detachment (for cohesive material), (2) affect the boundary shear stress induced by the main river flow (Yan Lu . et al. 2008). These two effects made by seepage force are not considered in the current study.

Fig.11 shows the distribution of pore water pressure and the free surface line and seepage velocity vectors at failure for the case of "Movable-bed" under the five flood hydrograph patterns. It is clear that the highest values of seepage velocities take place at the exit point near the toe of riverbank (as indicated by arrow size). In all patterns the seepage velocity vectors moves outward the bank except for Hyd-4 the seepage flow moves inward direction which emphasis the result obtained above that the failure occurs because of the geometry change, and not because of the pwp variation. Also, seepage flow is divided into two directions under the highest point on of GWT of Hyd-5 (point "m" Fig.11-e). This indicates that the recession rate is so fast that the GWT couldn't fall down uniformly along the whole bank

region and falls down near the bank making a hump shape.

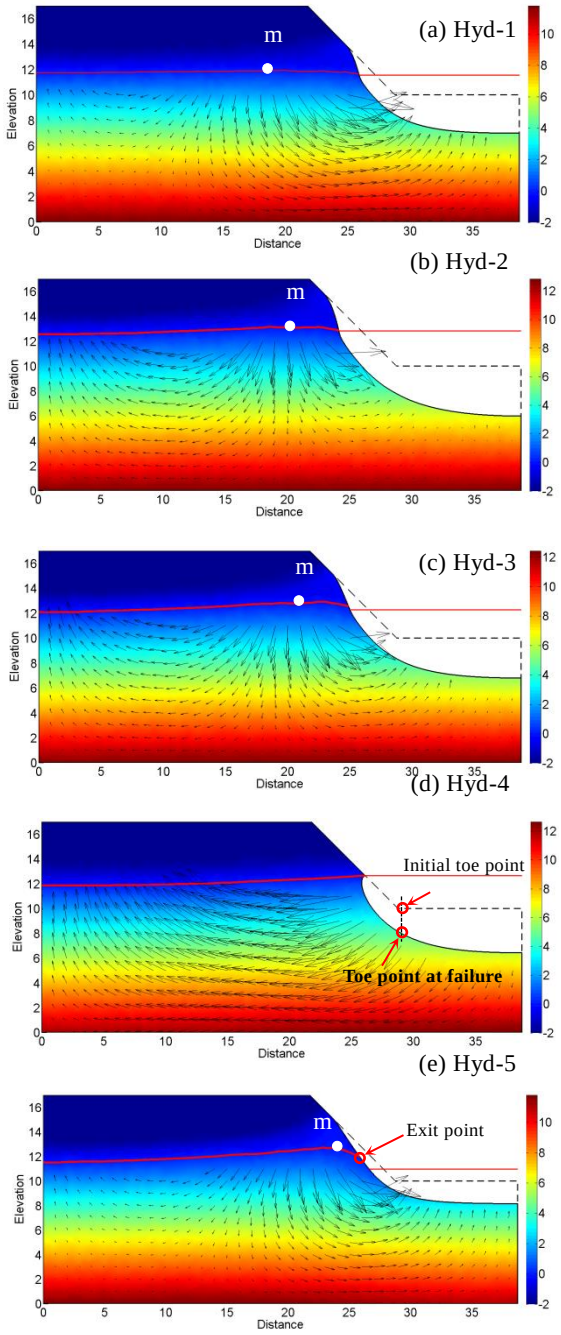

Fig.11 Free surface and seepage velocity vectors at failure for the case of " Movable-bed"

5. Conclusions

Current study has presented numerical study of riverbank response to various flood events. Five flood patterns were proposed to effect on the riverbank, three conditions of bed erosion have been investigated. A summary of key results is provided as follows:

1- By involving the three simulation models (erosion + seepage + stability), factor of safety, expected failure plane, collapse time, riverbank geometry, and pore water pressure could be successfully calculated for different flood hydrograph patterns.

2- Innovative idea of incorporating the lateral erosion in the stability analysis is applied. Here we add this model and it is very important to consider the eroded parts (and overhangs). The dynamic response is involved at every time step during the flood considering moving boundaries.

3- The process of lateral erosion increases the bed width of the channel and results in steepening of the bank, which reduces its stability. Bed lowering increases the bank height until a critical height is reached and the bank collapse.

4- The riverbank can restore back its stability as long as the water inside it is drained out.

5- The increase of water level in the river sustains the bank stability because the exerted hydrostatic pressures ensure a stabilizing factor.

6- The high pore water pressure is an adverse factor against riverbank stability.

7- The rate of change in the free-surface inside the bank controls its stability. The more drainable bank material, the more stable it is.

8- The simulated results show that riverbank failure is triggered particularly when during the falling stage, which has been pointed out by other researchers as well.

Acknowledgements

Authors would like to acknowledge the financial support from the Ministry of Education, Culture, Sports, Science and Technology (MEXT) of Japan.

References

Briaud, J. L., C. K. Ting, H. C. Chen, S. W. Han, K. W. Kwak (2001): Erosion function apparatus for scour rate predictions. J. Geotech. Geoenviron. Eng. 127(2),pp.105-113.

Griffiths, D.V., and P.A. Lane.(1999): Slope stability analysis by finite elements. Geotechnique, vol. 49, no. 3, pp. 387-403.

Langendoen, Eddy J., and Andrew Simon (2008): Modeling the evolution of incised streams. II: Stream bank erosion. Journal of hydraulic engineering.

Osman, A. M., and C. R. Thorne (1988) :Riverbank stability analysis I:Theory, J. Hydraul. Eng., 114, pp.134-150, doi:10.1061/(ASCE)0733-9429.

Rinaldi, Massimo, et al. (2004): Monitoring and modelling of pore water pressure changes and riverbank stability during flow events. Earth Surface Processes and Landforms 29.2, pp.237-254.

Van Genuchten, M. Th. (1980): A closed-form equation for predicting the hydraulic conductivity of unsaturated soils. Soil Science Society of America Journal 44, pp.892-898.

Aly El-Dien A., Takebayashi H., Fujita M. (2013) : Numerical model to estimate the fluvial hydraulic erosion in cohesive riverbanks. Proceedings of the 35th IAHR World Congress, China.

Darby, S. E., H. Q. Trieu, P. A. Carling, J. Sarkkula, J. Koponen, M. Kummu, I. Conlan, and J. Leyland (2010): Aphysically based model to predict hydraulic erosion of fine‐grained riverbanks: The role of form roughness in limiting erosion, J. Geophys. Res., 115, F04003.

Duncan, J. M. (1996): State of the art: limit equilibrium and finite-element analysis of slopes, Journal of Geotechnical engineering, 122(7), pp.577-596.

Fredlund, D. G., Anqing Xing (1994): Equations for the soil-water characteristic curve, Canadian Geotechnical Journal. Vol. 31, pp. 521-532.

Gottardi, G., and M. Venutelli, (2001) : UPF: two-dimensional finite-element groundwater flow model for saturated–unsaturated soils. Computers & geosciences 27.2

Guoliang Yu., and Soon-KeatTan., (2007) : Estimation of boundary shear stress distribution in open channels using flownet. Journal of Hydraulic Research 45, no. 4, pp. 486-496.

Hooke, J.M., (1979): An analysis of the processes of river bank erosion. Journal of Hydrology 42, pp.39–62.

Julian, Jason P., and Raymond Torres., (2006) Hydraulic erosion of cohesive riverbanks. Geomorphology 76.1, pp. 193-206.

Knighton, A.D., (1973): Riverbank erosion in relation to stream flow conditions, River Bollin-Dean, Cheshire. East Midland Geographer 6, pp. 416–426.

Lane, P. A., Griffiths D. V.(2000): Assessment of stability of slopes under drawdown conditions. Journal of geotechnical and geoenvironmental engineering 126, no. 5, pp. 443-450.

Matsui, T., San, K. (1992): Finite element slope stability analysis by shear strength reduction technique, Soils and Foundations, 32(1), pp.59-70.

Rinaldi, Massimo, and Stephen E. Darby.(2007): 9 Modelling river-bank-erosion processes and mass failure mechanisms: progress towards fully coupled simulations. Developments in Earth Surface Processes 11, pp. 213-239.

Smith, I. M., D. V. Griffiths, and L. Margetts (2013) : Programming the Finite Element Method. John Wiley & Sons.

Swan, C. C., Seo, Y. (1999): Limit state analysis of earthen slopes using dual continuum/FEM approaches." Int. J. Num. Anal. Meth.Geomech., 23(12), pp. 1359-1371.

Thome, C.R.,(1982): Processes and mechanisms of river bank erosion, in Gravel‐Bed Rivers: Fluvial Processes: Hey, R.D.. Bathurst, J.C., and Thorne, C.R. (EdS), Gravel-bed Rivers. Wiley. Chichester, pp. 227-271.

Wolman, M.G., (1959) : Factors influencing erosion of a cohesive riverbank. American Journal of Science 257,pp. 204-216.

Yan Lu a , Yee-Meng Chiew b & Nian-Sheng Cheng, (2008) : Review of seepage effects on turbulent open channel flow and sediment entrainment.

(Received June 11, 2015)